EPJ Web of Conferences **291**, 05010 (2024) https://doi.org/10.1051/epjconf/202429105010
MESON 2023

Electroproduction of Hypernuclei

Daria Denisova[1,2,*], *Petr* Bydžovský[1], *Petr* Veselý[1], and *Dalibor* Skoupil[1]

[1]Nuclear Physics Institute, Czech Academy of Sciences, Řež, Czech Republic
[2]Institute of Particle and Nuclear Physics, Faculty of Mathematics and Physics, Charles University, Prague, Czech Republic

Abstract. The electroproduction of hypernuclei initiates a captivating domain of study, offering great insights into the characteristics of composite nucleon-hyperon systems. This inquiry assumes prime significance as it displays critical features of nuclear matter structure and tests the interactions between hyperons and nucleons. In this paper, we unveil the distorted-wave impulse approximation (DWIA) approach, aimed at explaining the cross sections in electroproduction of Λ-hypernuclei. Our investigation examines how various model assumptions affect the results we get. We focus on two important factors: influence of the proton Fermi motion and description of the various models of nuclear and hypernuclear structure.

1 Introduction

Among various reactions employed for hypernucleus production [1, 2], electroproduction stands out as particularly intriguing. This is due to the well-understood nature of the electromagnetic interaction, which lends itself to perturbative treatment. In the specific kinematic conditions considered, i.e. involving substantial photon and kaon momenta ($\approx$ 1 GeV), the electroproduction reaction can be effectively described in the distorted-wave impulse approximation (DWIA) [3–5]. Furthermore, the advantageous energy resolution attainable in experiments utilizing electron beams surpasses that achievable in reactions induced by hadrons [2]. As a result, electroproduction enables the extraction of more precise insights into the reaction process and the intricate facets of the effective hyperon-nucleon interaction. The necessity of providing the specifications for the input parameters, including the elementary amplitude, structure calculations, and kaon distortion effects became apparent in a recent study [5], which emphasized the significance of Fermi motion and other kinematic effects in the electroproduction of hypernuclei.

The influence of Fermi motion effects was also explored previously [6] in the context of electromagnetic hypertriton production, utilizing the two-component form of the elementary production amplitude within a generalized reference frame. Employing the KAON-MAID [7] model for the elementary amplitude, the significant role of Fermi motion effects in accurately describing hypertriton electroproduction was underscored. Notably, in the work [6] the substantial effects in the longitudinal component of the cross section were observed, which aligns with our recent findings pertaining to heavier hypernuclei [5]. Consequently,here the optimal on-shell approximation is adopted, as discussed in [5], which incorporates Fermi

*e-mail: denisova.d.i95@gmail.com

motion to some extent through the proton's optimal momentum. This approach permits the utilization of the on-energy-shell elementary amplitude.

In previous works [3–5], we delved into the cross section for the electroproduction of p-shell hypernuclei using a phenomenological shell model. This model's nucleon-nucleon and effective YN interactions were meticulously tuned to precise data obtained from γ-ray spectroscopy [8]. Recently we studied the cross section of the electroproduction of various p-shell and sd-shell hypernuclei within two other many-body methods, namely TD_Λ and EMPM_Λ [9] to also provide predictions for the prepared experiment E12-15-008 at JLab on the ^{40}Ca and ^{48}Ca targets.

2 Approach

The construction of the elementary electroproduction amplitude is based on the assumption that the particles, except the virtual photon, are on their mass shell, and that energy-momentum conservation is maintained. However, in the impulse approximation , the initial proton and Λ are not considered asymptotically free particles. In our model calculations, we maintain that it is reasonable to keep the baryons on their mass shell and uphold translational invariance for both the elementary and overall amplitudes, as well as for the wave functions of the nuclear and hypernuclear systems. Calculating the magnitude of kaon three-momentum is done through energy conservation principles. The opportunity to select an effective proton momentum can be exploited, and we refer to this chosen value as the "optimum" proton momentum. In practice, we have an equation that relates the magnitude of proton momentum and the angle with respect to the momentum transfer (Δ), allowing us to make a suitable choice.

Another focus of our work is on the electroproduction cross sections of the *p*- and *sd*-shell hypernuclei. The cross sections are calculated by using various (hyper)nuclear structure methods and interactions between baryons. The calculations are performed in the DWIA employing two elementary amplitudes for production of Λ hyperons. The one-body density matrix elements (OBDME) used in these calculations [5] are obtained within the nucleon-Λ Tamm-Dancoff approximation and EMPM_Λ [9]. These computations utilize the chiral NNLO_{sat} NN+NNN potential and the effective Nijmegen-F YN interaction. We discuss the exitation spectra in dependence of the structure models and interactions.

3 Results

In Figure 1 we illustrate the angular dependence of the electroproduction cross sections for the excited states $J^P = 1^+$, 2^+, and 3^+ of $^{12}_{\Lambda}$B. These results were obtained using the DWIA and the elementary amplitude BS3 [10]. The nuclear-hypernuclear structure, described by OBDME, is from the shell-model calculations following the work by Millener [8].

The calculations were performed under several scenarios, including the proton and Λ-frozen approximations, as well as the optimum on-shell approximation, using different kaon momenta, as discussed earlier. Notably, the results exhibit greater disparities for very small kaon angles, with the Λ-frozen approximation typically yielding larger values compared to the other approaches. This suggests that effects from the proton Fermi motion contribute to differences in the DWIA calculations, with variations up to approximately 10-20% observed for the dominant 3^+ hypernucleus state.

Additionally, it is worth mentioning that the optimum and frozen-proton approximations curves show distinct orders for the states 1^+ and 3^+, as well as for 2^+. These differences are primarily attributed to selective contributions from the longitudinal part of the electroproduction amplitude.

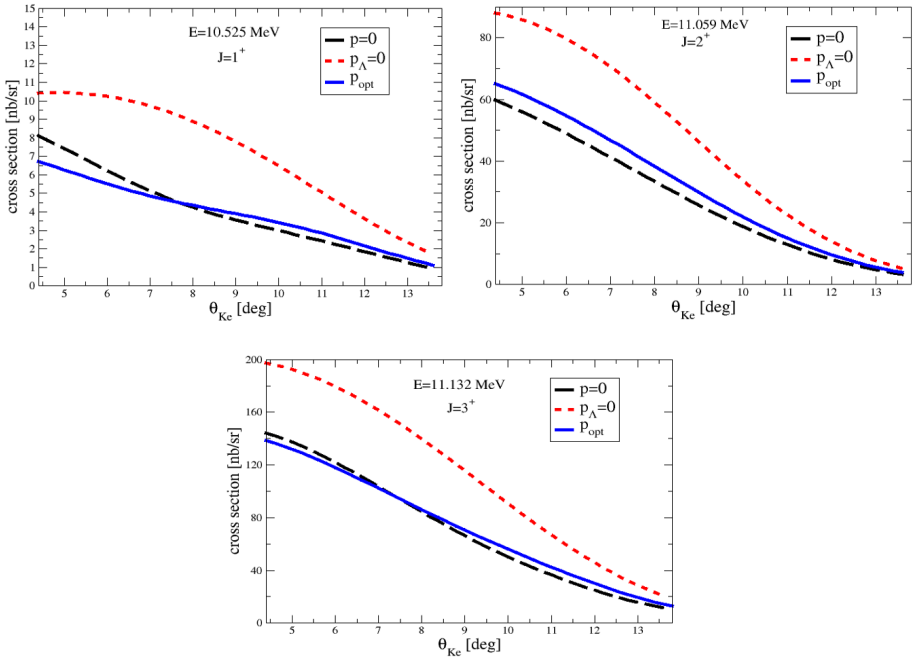

Figure 1. Angular dependence of the cross sections in electroproduction of ${}^{12}_{\Lambda}$B for three excited states. These states are characterized by their energy (E) and spin-parity (J^P). Results for various values of the proton effective momentum are compared.

In Figure 2, we present a comparison of the energy distributions of the cross section obtained in the TD_Λ and $EMPM_\Lambda$ [9] approaches with the data generated by the E94-107 experiment [3] and analyzed within a shell model framework [8]. Our TD_Λ and $EMPM_\Lambda$ calculations were done using the self-consistent HF basis and are parameter-free, except for the Fermi momentum k_F and the technical parameters, the initial harmonic oscillator (HO) basis-oscillator constant $\hbar\omega$ and the maximal number of oscillator shells N_{max}. In these calculations we employed the $NNLO_{sat}$ NN+NNN potential and the NF YNG interaction with Fermi momentum $k_F = 1.1\ fm^{-1}$.

On the left panel of Figure 2 with the excitation energy spectrum of ${}^{12}_{\Lambda}$B we compare the shell model [3], TD_Λ and $EMPM_\Lambda$ [9] approaches.The TD_Λ result successfully reproduce the two principal peaks , but it lacks the observed strength in between them. The inclusion of the TD_Λ configurations coupled to the excitations of the nuclear core in $EMPM_\Lambda$ results in a damping effect on the two main peaks aligning well with the data. Also there occurs additional peaks in between the two main ones, although they are of insufficient strength and not in the same energies as the experimentally observed bumps. In ${}^{16}_{\Lambda}$N the TD_Λ reproduce quite well the four peaks observed in the experimental spectrum. The incorrect positions of the 2nd and 4th peaks can be, in principle, corrected by enchancing the strength of the three-nucleon (NNN) force by 20% as shown in Figure 2. The corrected result coincides very well with the shell model result. However, changing the NNN force can also affect description of the other data, especially those used in determination of paramters of the $NNLO_{sat}$ potential.

More discussion of these methods and the details of our calculations can be found in [9].

4 Summary and outlook

A comprehensive two-component form of the elementary amplitude was formulated and utilized to demonstrate sensitivity of the cross section to the proton Fermi motion within the target nucleus. The impact of Fermi motion is particularly significant, notably in the longitudinal cross sections, especially at lower angles and energies exceeding 2 GeV.

The efficacy of the TD_Λ and $EMPM_\Lambda$ approaches employing Nijmegen YN and $NNLO_{sat}$ interactions was demonstrated in successfully describing experimental data for p-shell hypernuclei. These approaches yielded results consistent with those obtained through shell-model calculations. Consequently, formalism of TD_Λ and $EMPM_\Lambda$ is suitable for predicting excitation spectra of medium-mass hypernuclei [9], a task aligned with an upcoming planned experiment E12-15-008 at JLab.

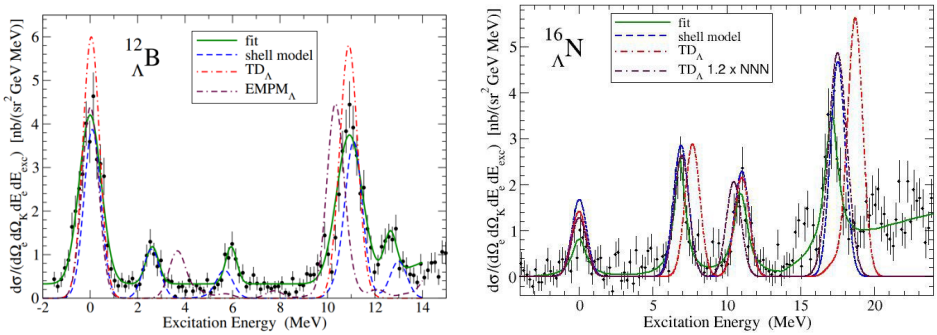

Figure 2. Excitation-energy spectra of $^{12}_{\Lambda}$B and $^{16}_{\Lambda}$N calculated with the elementary amplitude BS3 in the optimum on-shell approximation are compared with the data and a fit to the data [3]. The theoretical results are obtained within various approaches and interactions among baryons. In the case of $^{16}_{\Lambda}$N we also show the effect from a reinforcement of the NNN force by the factor 1.2.

References

[1] A. Gal, E.V. Hungerford, and D.J. Millener, Rev. Mod. Phys. **88**, 035004 (2016).
[2] O. Hashimoto and H. Tamura, Prog. Part. Nucl. Phys. **57**, 564 (2006).
[3] F. Garibaldi et al, Phys. Rev. C **99**, 054309 (2019).
[4] P. Bydžovský, D.J. Millener, F. Garibaldi, and G.M. Urciuoli, AIP Conf. Proc. **2130**, 020014 (2019).
[5] P. Bydžovský, D. Denisova, D. Skoupil, and P. Veselý, Phys. Rev. C **106**, 044609 (2022).
[6] T. Mart and B.I.S. van der Ventel, Phys. Rev. C **78**, 014004 (2008).
[7] T. Mart, C. Bennhold, H. Haberzettl, and L. Tiator, http://www.kph.uni-mainz.de/MAID/kaon/.
[8] D.J. Millener, Nucl. Phys. A **804**, 84 (2008); **835**, 11 (2010); **881**, 298 (2012).
[9] P. Bydžovský, D. Denisova, D. Petrellis, D. Skoupil, P. Veselý, G. De Gregorio, F. Knapp, and N. Lo Iudice, Phys. Rev. C **108**, 024615 (2023).
[10] D. Skoupil, P. Bydžovský, Phys. Rev. C **97**, 025202 (2018).